COMPUTER METHODS AND PROGRAMS IN BIOMEDICINE XXX (2014) XXX–XXX

journal homepage: www.intl.elsevierhealth.com/journals/cmpb

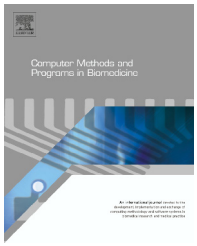

A heterogeneous coupled oscillator model for simulation of ECG signals

*E. Ryzhii, M. Ryzhii**

Complex Systems Modeling Laboratory, University of Aizu, Aizu-Wakamatsu 965-8580, Japan

ARTICLE INFO

Article history:
Received 27 January 2014
Received in revised form
25 March 2014
Accepted 16 April 2014

Keywords:
Delay differential equations
MATLAB
ECG
Heart model
van der Pol
FitzHugh–Nagumo

ABSTRACT

We present a novel model of cardiac conduction system including main pacemakers and heart muscles. Sinoatrial node, atrioventricular node and His–Purkinje system are represented by modified van der Pol-type oscillators connected with time-delay velocity coupling. For description of atrial and ventricular muscles, where depolarization and repolarization processes are considered as separate waves, we use modified FitzHugh–Nagumo model. In this work, we obtained synthetic ECG as a combined signal of atrial and ventricular muscles and reproduced several normal and pathological rhythms. Inclusion of cardiac muscle response allows to investigate interactions between pacemakers and resulting global heartbeat dynamics by means of clinically comparable realistic ECG signals. This feature distinguishes our model from existing cardiac oscillator models. To solve the system of differential equations describing the proposed heterogeneous coupled oscillator model we developed a software in MATLAB environment utilizing special DDE23 function.

1. Introduction

Nowadays, computer modeling of cardiac electrophysiology became very important in understanding real processes taking place in healthy and diseased hearts. The most well known and widely used in clinical and theoretical research set of physiological signals produced by electrical activity of the heart is electrocardiogram (ECG). The ECG is a record of electric potentials generated by the heart on the body surface because of propagation of activation and recovery waves through cardiac muscle tissue. The nonlinear analysis of ECG signals is commonly used in studies of cardiac and cardiovascular diseases [1–3].

For the modeling of the electrical processes in the heart, various modeling approaches with different levels of details have been proposed and utilized. The majority of the models describe functioning of the heart on the cellular level, obtaining propagation of action potentials among cardiomyocytes. Simulations on 2D or 3D tissue slabs produce pseudo electrograms [4,5], while 3D biventricular, atrial or whole-heart models coupled with torso model can yield more realistic ECG signals. These models are based on either rule-based (cellular automaton) or reaction–diffusion (see, for example, [6,7] and references wherein) approaches for simulation of excitation waves propagation. The latter approach usually requires a lot of computational resources to solve huge number of differential equations for ionic currents in cell membranes with many parameters.

There is a different class of models, which describe of heartbeat dynamics in general with a set of ordinary differential equations. Some of the models generate synthetic ECG

* *Corresponding author*. Tel.: +81 242372566.
E-mail addresses: eryzhii@hotmail.com (E. Ryzhii), m-ryzhii@ieee.org, mryzhii@yahoo.com (M. Ryzhii).

http://dx.doi.org/10.1016/j.cmpb.2014.04.009
0169-2607/

signals using a dynamical system on a circle [8–11] without taking into account structure of the cardiac conduction system. In other models the heart is compartmentalized into separate elements such as natural cardiac pacemakers only [12–25] or pacemakers and muscles [26–28] using different modifications of the coupled van der Pol (VDP) type nonlinear relaxation oscillators [29]. Utilization of the modified VDP oscillators allows adoption of their intrinsic frequencies to the driving signal without significantly changing the amplitude, which corresponds to the real interactions between natural cardiac pacemakers. Most of the above-mentioned oscillator models are focused on the generation of transmembrane action potentials and the study of their synchronization, bifurcation and chaos, but only a few are intended for calculation of realistic ECG.

The model proposed by Gois et al. [22] allows generating electrical response of main cardiac pacemakers and obtaining the ECG as a composition these signals. The disadvantage of the model is that in reality the pacemakers signals are rather weak in comparison with the cardiac muscle ones, and do not significantly contribute to the aggregated ECG signal. On the other hand, the responses of atrial and ventricular muscles, which actually produce the main input, were not included in this model. To eliminate this drawback, we recently proposed to incorporate into the system quiescent excitable FitzHugh–Nagumo-type (FHN) oscillators for accurate description on the cardiac muscle electrical responses [30].

In the present work, we further developed our model and pertinent software with inclusion of a description for depolarization and repolarization waves in the atria and ventricles utilizing separate modified FHN systems for each of the processes, which allows generating physiologically correct ECG signals.

2. Cardiac conduction system

The cardiac conduction system is a group of specialized cells in the walls of the heart that send signals to the cardiac muscles causing them to contract (Fig. 1). The electrical impulse originates in the sinoatrial (SA) node situated in the right atrium and stimulated by autonomous nervous system [31]. The impulse first initiates a depolarization (activation) wavefront that propagates through atrial (AT) muscle resulting in its contraction.

The electrical signal is subsequently delayed in the atrioventricular (AV) node, located in the boundary between atria and ventricles (VN), to allow the atrial muscles to complete the contraction and to fill the ventricular chambers with blood. The AV node at its turn fires the impulse which travels rapidly through the fibers of His–Purkinje (HP) system to the ventricles. The impulse triggers a depolarization wavefront in the ventricles, which results in their efficient contraction, pumping blood throughout the body.

Under normal conditions, the SA node generates electrical impulses with a rate of 60–80 beats per minute (bpm) at rest. If the SA node fails to create an impulse, then the AV node can take over as the main pacemaker and stimulate the heart at the intrinsic rate of about 40–60 bpm. Further, if no excitation signal is delivered from the both SA and AV pacemakers, the HP cells can fire at its own rate of about 20–40 bpm [32].

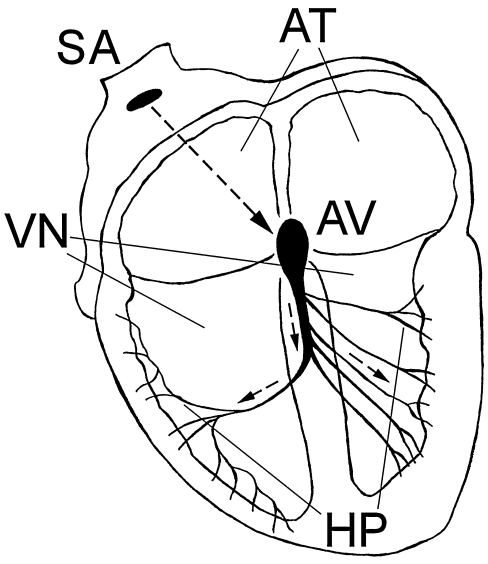

Fig. 1 – Cardiac conduction system.

During every heart beat the electrical impulse propagates from one muscle cell to the next adjacent cell until the whole atria and ventricles are depolarized. After each heart muscle region has excited, a process of repolarization (recovery) is initiated, permitting cardiac cells to depolarize again at the arrival of the next stimulation impulse.

The general behavior of atrial and ventricular electrical activity is recorded as body surface ECG waveforms. Atrial depolarization and repolarization are recorded on the ECG as P and Ta (atrial T) waves, respectively [31]. The depolarization of ventricles is reflected on the ECG by the QRS complex. Since atrial repolarization generally occurs at the same time as ventricular depolarization and is much smaller in amplitude, normally the Ta wave is merged with QRS complex, and thus not recorded as a separate wave. Nevertheless, it can become visible in some pathological situations, for example, complete AV block. The T wave corresponds to ventricular repolarization, and generally takes more time to complete than the QRS complex.

The macroscopic structure of the cardiac conduction system described above formed the basis of our proposed heterogeneous oscillator model for calculation of ECG signals. General scheme of the model is shown in Fig. 2. In addition to three coupled oscillator system based on modified VDP equations, we consider the depolarization and repolarization wavefronts in the atrial and ventricular muscles as separate processes, each individually presented by an excitable FHN system. The detailed mathematical description of the oscillating pacemaker (SA–AV–HP) and quiescent excitable muscle (AT and VN) systems follows separately below.

Please cite this article in press as: E. Ryzhii, M. Ryzhii, A heterogeneous coupled oscillator model for simulation of ECG signals, Comput. Methods Programs Biomed. (2014), http://dx.doi.org/10.1016/j.cmpb.2014.04.009

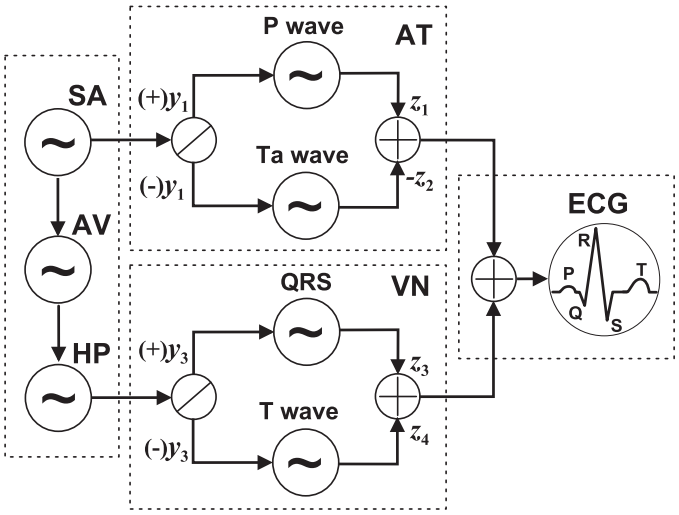

Fig. 2 – General scheme of the heart model.

3. Mathematical model

3.1. *Modified VDP model for natural cardiac pacemakers*

The VDP model [29] has been widely used in theoretical studies of the heart electrical activity. The standard VDP relaxation oscillator equation is given by the following Liénard planar system:

$$\begin{aligned}\dot{x} &= y\\ \dot{y} &= -F(x)y - G(x),\end{aligned} \tag{1}$$

where

$$F(x) = \alpha(x^2 - u), \quad G(x) = \omega^2 x, \tag{2}$$

$\alpha > 0$ and $u = 1$ are the factors representing nonlinear damping force, ω is the intrinsic natural frequency of the oscillator, and $x(t)$ corresponds to the amplitude of the heart electrical signal, which is related to the cardiac action potential.

Considering the features of neuronal oscillator models, such as Morris–Lecar model [33], Postnov et al. [34] proposed a simple oscillator model that is easily controllable and that still reproduces the behavior of the neuronal oscillators. Modifying the standard VDP equation, the authors replaced the linear harmonic force $G(x)$ to cubic Duffing nonlinear term $x(x+d)(x+2d)/d^2$ to maintain the features of the oscillator phase space similar to neuronal one, which includes three equilibrium points – the focus, the saddle, and the stable node.

The model was further improved by Grudzinski and Zebrowski [17], who investigated its adaptation for simulation of cardiac pacemaker behavior. To enhance the potential of the model, they changed the dumping term $F(x)$ to asymmetric form with respect to the variable x and introduced independent parameters d and e in the force term $G(x)$ for the position control of hyperbolic saddle and stable node, respectively:

$$F(x) = \alpha(x - u_1)(x - u_2), \quad G(x) = \omega^2 x(x + d)(x + e), \tag{3}$$

where the product $u_1 u_2$ should be negative to keep the self-oscillatory property of the system. The utilization of Eq. (3) allows modeling of general behavior of cardiac pacemakers and reproduction of some cardiac phenomena [17,27].

One of the most universal features describing the behavior of interacting oscillator systems is synchronization. It manifests as an adjustment of rhythms (phase-locking with nonzero constant phase shift) due to an interaction between two or more oscillators, and does not necessarily require complete temporal coincidence of signals. To provide the interaction in the systems, proper coupling should be set up between the oscillators or pacemaker nodes. A diffusive coupling (nearest-neighbor local coupling) is the most common type of coupling present in physical and biological systems. In the diffusively coupled system, generally coupling terms should include both differences: $(x_i - x_{i-1})$ for position coupling and $(y_i - y_{i-1})$ for velocity coupling, which, in application to the heart system, correspond to the coupling by potential and current, respectively. As a result, an element $i > 1$ in the unidirectionally coupled oscillator array may look as follows [34]:

$$\begin{aligned}\dot{x}_i &= y_i + K_{x_i}(x_i - x_{i-1})\\ \dot{y}_i &= -F_i(x)y_i - G_i(x) + K_{y_i}(y_i - y_{i-1}),\end{aligned} \tag{4}$$

where K_i are the coupling coefficients. However, a number of diffusive coupling method variations can be found in the literature (see, for example, [16,19,20,23,35]). The asymmetric position-only coupling added to the first equation of (4) was used in the spatially dimensional SA–AV model [17], while in the work [22] this coupling term with time delays was added to the second equation. Performing a number of simulations on a system with position-variable coupling added to the

Please cite this article in press as: E. Ryzhii, M. Ryzhii, A heterogeneous coupled oscillator model for simulation of ECG signals, Comput. Methods Programs Biomed. (2014), http://dx.doi.org/10.1016/j.cmpb.2014.04.009

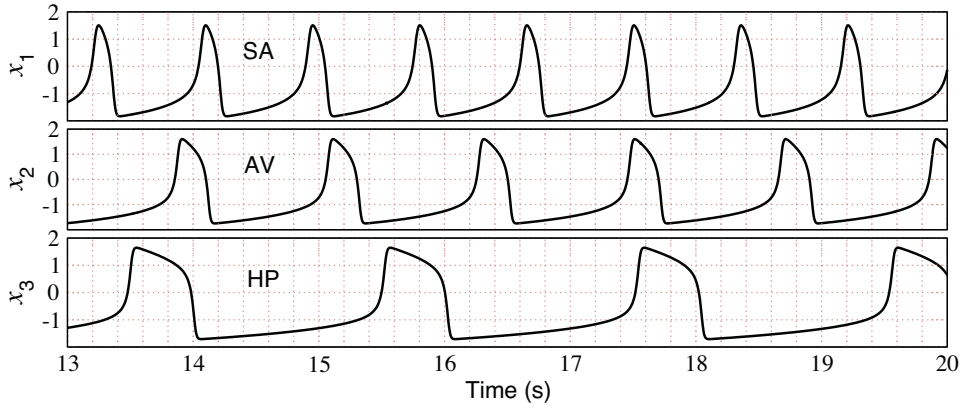

Fig. 3 – Calculated action potentials of uncoupled pacemakes at their intrinsic firing rates.

right-hand side of the second equation of (4) similar to the three cardiac oscillator system (SA–AV–HP) described in Ref. [22], we found that synchronization level is not enough in wide range of beat rates (30–200 bpm). In particular, the synchronization problem occurred at very high sinus rates (>140 bpm) in the HP oscillator node, which has the lowest intrinsic rate (35 bpm). The application of the velocity coupling to the right-hand side of the second equation significantly improved in-phase synchronization at such high rates [35]. Moreover, it is also known that the synchronization level depends on the coupling coefficients K as well [18].

Taking into account the above-mentioned considerations, in our proposed mathematical model we describe all three natural pacemakers by a system of modified asymmetric VDP equations with unidirectional time-delay velocity coupling only:

$$SN\begin{cases}\dot{x}_1 = y_1\\ \dot{y}_1 = -a_1 y_1(x_1-u_{11})(x_1-u_{12}) - f_1 x_1(x_1+d_1)(x_1+e_1).\end{cases} \tag{5}$$

$$AV\begin{cases}\dot{x}_2 = y_2\\ \dot{y}_2 = -a_2 y_2(x_2-u_{21})(x_2-u_{22}) - f_2 x_2(x_2+d_2)(x_2+e_2)\\ \quad + K_{SA-AV}(y_1^{\tau_{SA-AV}} - y_2),\end{cases} \tag{6}$$

$$HP\begin{cases}\dot{x}_3 = y_3\\ \dot{y}_3 = -a_3 y_3(x_3-u_{31})(x_3-u_{32})\\ \quad - f_3 x_3(x_3+d_3)(x_3+e_3) + K_{AV-HP}(y_2^{\tau_{AV-HP}} - y_3).\end{cases} \tag{7}$$

Here indexes SA–AV and AV–HP of the coupling coefficients represent unidirectional coupling between the pacemakers, $y_i^{\tau_n} \equiv y_i(t-\tau_n)$ are the velocity coupling components of the time-delay signal, and τ_n are the corresponding time delays.

The parameters a_i, d_i, e_i, f_i, and u_i for (5)–(7) were selected to obtain intrinsic oscillation rates of 70 bpm, 50 bpm, and 35 bpm for uncoupled SA, AV, and HP oscillators, respectively, and with shapes close to experimental data on action potentials of real pacemakers [36–38]: $a_1 = 40$, $a_2 = a_3 = 50$, $u_{11} = u_{21} = u_{31} = 0.83$, $u_{12} = u_{22} = u_{32} = -0.83$, $f_1 = 22$ for normal sinus rhythm of 70 bpm, $f_2 = 8.4$, $f_3 = 1.5$, $d_1 = d_2 = d_3 = 3$, $e_1 = 3.5$, $e_2 = 5$, and $e_3 = 12$. The resulting action potentials of the uncoupled pacemakers firing at their intrinsic rates are shown in Fig. 3. We found that to maintain stable synchronization between the oscillators with change of the SA rate, the coupling coefficients should be proportional to $\omega_1^2 \sim f_1$, thus for simplicity we set $K_{SA-AV} = K_{AV-HP} = f_1$.

3.2. *Modified FHN model for cardiac muscles*

In contrast to the properties of the pacemaker cells, cardiac muscle cells does not demonstrate self-oscillatory behavior. They have to be stimulated by an electrical signal from a pacemaker to produce a single response, i.e depolarization, which leads to their contraction. For simulation of atrial and ventricular muscles an equation for quiescent excitable element, such as modified FHN model or VDP model with positive product $u_1 u_2$ [26], is necessary to adequately describe electrical response. These models have a low level stable oscillatory state for small values of applied stimulating current.

In our proposed model of cardiac conduction system, the description of electrical responses of cardiac muscles on a stimulation by pacemakers in both atria and ventricles is based on FHN class model [39,40] for excitable media:

$$\begin{aligned}\dot{z} &= -cz(z-w_1)(z-w_2) - bv + I\\ \dot{v} &= h(z-gv).\end{aligned} \tag{8}$$

Here z is the excitation variable corresponding to the net transmembrane potential of all cells of the muscle, and v is the recovery variable (quantity of refractoriness). The cubic term in the first equation controls the activation, parameter c defines the amplitude of the pulse, and parameters $w_1 < w_2$ represent excitation threshold and excited state, respectively. Parameters b and g change the rest state and dynamics, h represents excitability and controls the abruptness of activation and the duration of the action potential, and I is the magnitude of stimulation current.

Different variations of these equations can be found in literature and sometimes also called as Bonhoeffer–van der Pol model. The model is commonly used to describe different biological mechanisms and is able to reproduce many qualitative

Please cite this article in press as: E. Ryzhii, M. Ryzhii, A heterogeneous coupled oscillator model for simulation of ECG signals, Comput. Methods Programs Biomed. (2014), http://dx.doi.org/10.1016/j.cmpb.2014.04.009

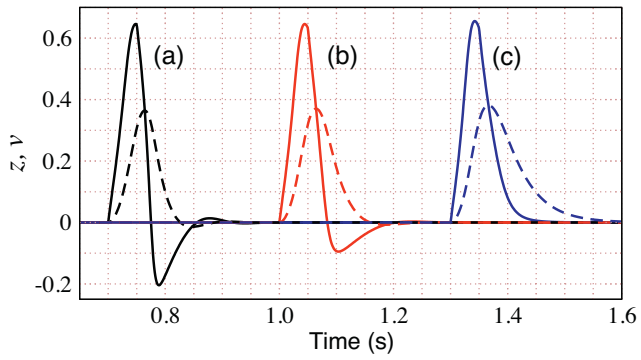

Fig. 4 – Response of the unmodified (a) and modified (b and c) FitzHugh–Nagumo systems on instantaneous stimulating current pulse. Solid and dashed curves correspond to the potential z and the recovery variable v, respectively.

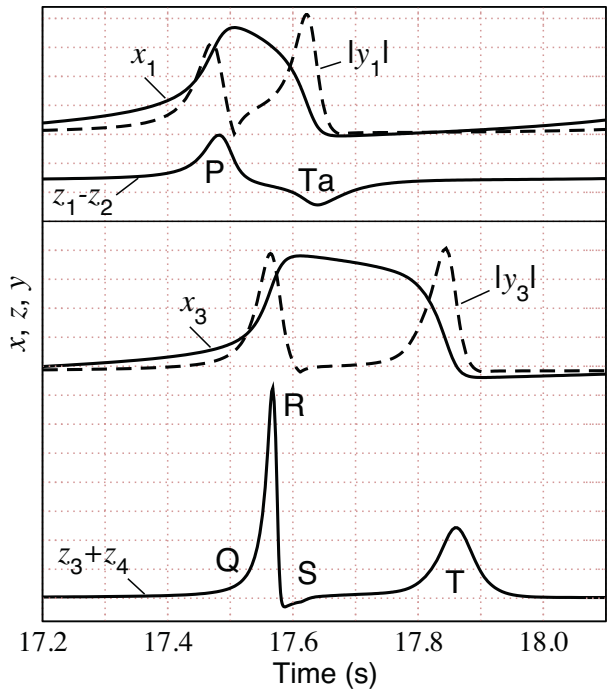

Fig. 5 – Coupling between pacemakers and muscles. Calculated action potentials (x_i), absolute value of their derivatives (y_i), and muscle response (z_i) for sinoatrial pacemaker and atrium muscle (top panel), and His–Purkinje pacemaker and ventricular muscle (bottom panel).

characteristics of excitable media such as excitation threshold, relative and absolute refractory periods.

The standard FHN system produces hyperpolarization of z – its value becomes negative at the beginning of the refractory period (see Fig. 4(a)), which is undesirable for many applications of the model. Rogers et al. [41] proposed to eliminate the hyperpolarization by replacing the term bv in the first equation to bvz (thus, adding the nullcline $z=0$ to the phase plane) as shown in Fig. 4(c). However, in our case an undershoot of z can be useful for representation of the S wave in the QRS complex. To control the negative excursion of z we use both original and modified terms in the right side of the first equation of (8):

$$\begin{aligned} \dot{z} &= -cz(z-w_1)(z-w_2) - bv - dvz + I \\ \dot{v} &= h(z-gv). \end{aligned} \tag{9}$$

The examples of the resulting waveforms for three sets of parameters are shown in Fig. 4. Curve (a) corresponds to unmodified FHN system – $b=174$, $d=0$, curve (b) – to the modified system with $b=105$, $d=45$, and curve (c) – to the modified system with $b=0$ and $d=105$. The latter corresponds to the modification proposed in [41]. Other parameters for Fig. 4 are as follows: $c=300$, $w_1=0.12$, $w_2=0.8$, $h=24$, $g=1$, and the amplitude of the instantaneous current pulse $I(t)=I_0\delta(t)$ was $I_0=15$.

Using the proposed quiescent excitable FHN model (9) we describe the depolarization and repolarization processes in cardiac muscles as a system of four sets of ordinary differential equations:

$$\text{P wave} \begin{cases} \dot{z}_1 = k_1(-c_1z_1(z_1-w_{11})(z_1-w_{12}) \\ \quad -b_1v_1 - d_1v_1z_1 + I_{AT_{De}}) \\ \dot{v}_1 = k_1h_1(z_1-g_1v_1), \end{cases} \tag{10}$$

$$\text{Ta wave} \begin{cases} \dot{z}_2 = k_2(-c_2z_2(z_2-w_{21})(z_2-w_{22}) \\ \quad -b_2v_2 - d_2v_2z_2 + I_{AT_{Re}}) \\ \dot{v}_2 = k_2h_2(z_2-g_2v_2), \end{cases} \tag{11}$$

for AT muscles and

$$\text{QRS} \begin{cases} \dot{z}_3 = k_3(-c_3z_3(z_3-w_{31})(z_3-w_{32}) \\ \quad -b_3v_3 - d_3v_3z_3 + I_{VN_{De}}) \\ \dot{v}_3 = k_3h_3(z_3-g_3v_3), \end{cases} \tag{12}$$

$$\text{T wave} \begin{cases} \dot{z}_4 = k_4(-c_4z_4(z_4-w_{41})(z_4-w_{42}) \\ \quad -b_4v_4 - d_4v_4z_4 + I_{VN_{Re}}) \\ \dot{v}_4 = k_4h_4(z_4-g_4v_4), \end{cases} \tag{13}$$

for VN muscles, respectively, where k_i are the scaling coefficients. The values of the parameters for Eqs. (10)–(13) are the following: $k_1=2\times10^3$, $k_2=4\times10^2$, $k_3=10^4$, $k_4=2\times10^3$, $c_1=c_2=0.26$, $c_3=0.12$, $c_4=0.1$, $b_1=b_2=b_4=0$, $b_3=0.015$, $d_1=d_2=0.4$, $d_3=0.09$, $d_4=0.1$, $h_1=h_2=0.004$, $h_3=h_4=0.008$, $g_1=g_2=g_3=g_4=1$, $w_{11}=0.13$, $w_{12}=w_{22}=1.0$, $w_{21}=0.19$, $w_{31}=0.12$, $w_{32}=1.1$, $w_{41}=0.22$, $w_{42}=0.8$. We selected the parameter values in such a way to obtain pronounced difference between relatively fast depolarization (high and narrow P and R waves) and slow repolarization (low and wide Ta and T waves) processes.

The stimulation impulses of the transmembrane ionic currents I represent the couplings between the SA and HP pacemakers and AT and VN muscles, respectively, provided by corresponding current pulses (Fig. 2). For the latter we use

Please cite this article in press as: E. Ryzhii, M. Ryzhii, A heterogeneous coupled oscillator model for simulation of ECG signals, Comput. Methods Programs Biomed. (2014), http://dx.doi.org/10.1016/j.cmpb.2014.04.009

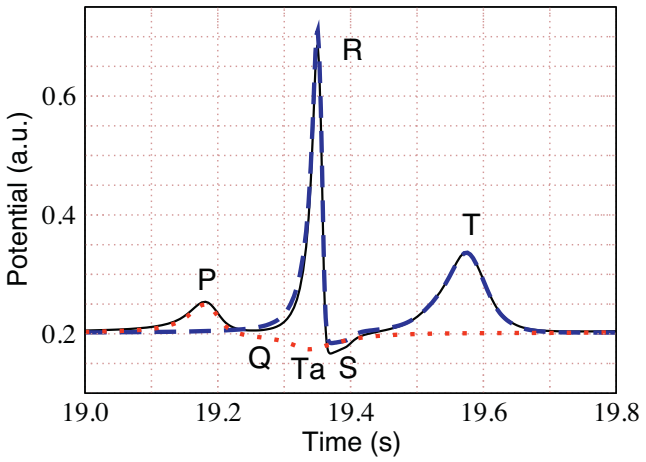

Fig. 6 – Atrial (dotted line), ventricular (dashed line), and net ECG (solid line) waveforms for normal case (see also Fig. 7).

absolute values of y_1 and y_3 (see Fig. 5), and calculate amplitudes of the stimulation current pulses as follows:

$$I_{AT_{De}} = \begin{cases} 0, & \text{for } y_1 \le 0 \\ K_{AT_{De}} y_1, & \text{for } y_1 > 0 \end{cases}$$

$$I_{AT_{Re}} = \begin{cases} -K_{AT_{Re}} y_1, & \text{for } y_1 \le 0 \\ 0, & \text{for } y_1 > 0 \end{cases}$$

$$I_{VN_{De}} = \begin{cases} 0, & \text{for } y_3 \le 0 \\ K_{VN_{De}} y_3, & \text{for } y_3 > 0 \end{cases}$$

$$I_{VN_{Re}} = \begin{cases} -K_{VN_{Re}} y_3, & \text{for } y_3 \le 0 \\ 0, & \text{for } y_3 > 0 \end{cases}$$

Here the coefficients were selected as follows: $K_{AT_{De}} = 4 \times 10^{-5}$, $K_{AT_{Re}} = 4 \times 10^{-5}$, $K_{VN_{De}} = 9 \times 10^{-5}$, and $K_{VN_{Re}} = 6 \times 10^{-5}$.

3.3. *Calculation of the combined ECG signal*

The total synthetic ECG waveform is calculated as a composition of the signals from AT and VN muscles (see Figs. 5 and 6):

$$ECG = z_0 + z_1 - z_2 + z_3 + z_4. \quad (14)$$

Here, we adjusted the parameter $z_0 = 0.2$ to provide zero baseline of the ECG signal. The value of z_2 which corresponds to atrial Ta wave is added with negative sign due to the fact that it is known to be opposite to P wave [31].

Numerical simulations with the proposed model were performed in MATLAB environment employing DDE23 function [42,43] for calculation of the delay differential equations. The DDE23 solver makes the solution of wide range of delay differential equations as easy as possible in many research areas, for example, in computational pharmacokinetics [44].

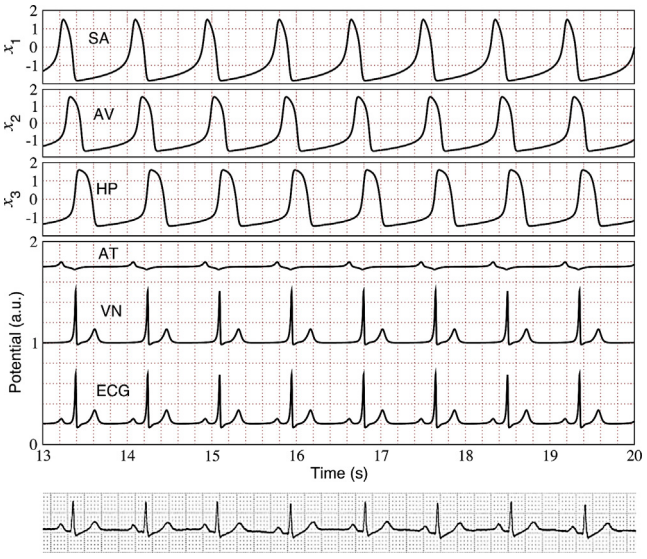

Fig. 7 – Calculated action potentials, muscle response and ECG at 70 bpm (normal case) and real patient's ECG [45].

Since standard DDE23 function does not allow direct utilization of time-delay derivatives, we obtain them for Eqs. (6)–(7) in the following way:

$$y^{\tau} = \frac{x^{\tau_a} - x^{\tau_b}}{\tau_b - \tau_a} = \frac{x(t-\tau_a) - x(t-\tau_b)}{\tau_b - \tau_a}, \quad (15)$$

where $\tau = (\tau_a + \tau_b)/2$ is the desirable delay and $\tau_b - \tau_a = 0.05$ s.

We approximated the dependence of the total delay between coupled SA and HP nodes on the parameter f_1 as

$$\tau_{SA-HP} = \tau_{SA-AV} + \tau_{AV-HP} = 2.29/f_1 + 0.08. \quad (16)$$

Such dependence allows keeping the ratio of P–R and R–T intervals in physiologically correct range [31]. For simplicity, in all simulations performed in this work we set up equal delays of $\tau_{SA-HP}/2$ in both SA–AV and AV–HP conduction pathways without any effect to the resulting ECG. Thus, for normal rhythm of 70 bpm we have $\tau_{SA-AV} = \tau_{AV-HP} = 0.092$ s.

4. Results and discussion

To validate the proposed model, we performed a number of numerical simulations with different normal and pathological rhythms, shown in Figs. 7–11. The figures demonstrate calculated action potentials of SA, AV, and HP pacemakers, corresponding responses from AT and VN muscles, and resulting total ECG waveforms. The latter are presented in comparison with real patient's ECG (standard Einthoven lead II) [45,46].

For the normal case (see Fig. 7), all pacemakers are dominated by SA node and follow its rhythm of 70 bpm ($f_1 = 22$). The atrial and ventricular muscles are operating consequentially, so the positive P wave precedes the QRS complex, followed by the positive T wave, while the Ta wave is merged with the QRS complex.

After getting normal ECG as a reference, we tested our model by reproducing several well-known rhythm disorders.

Please cite this article in press as: E. Ryzhii, M. Ryzhii, A heterogeneous coupled oscillator model for simulation of ECG signals, Comput. Methods Programs Biomed. (2014), http://dx.doi.org/10.1016/j.cmpb.2014.04.009

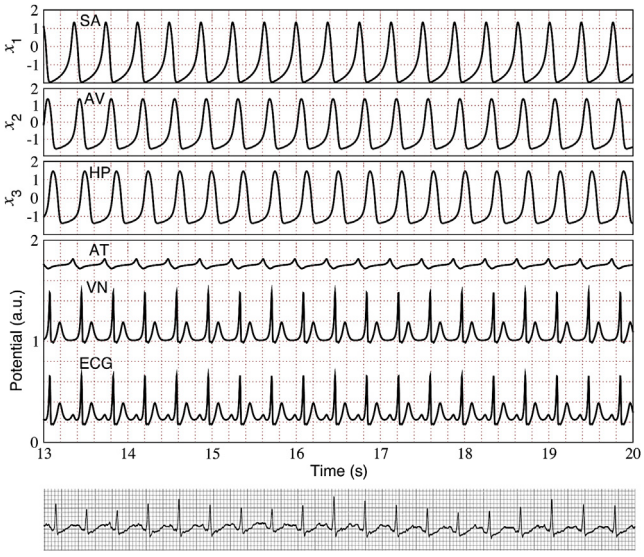

Fig. 8 – Calculated action potentials, muscle response and ECG at 160 bpm (tachycardia) and real patient's ECG [46].

We started with sinus tachycardia, the fast rhythm when SA node generates impulses greater than 100 bpm (in our case 160 bpm with $f_1 = 87$) with other pacemakers synchronously following this rate (Fig. 8). The rhythm is regular, but action potentials of all pacemakers became shorter with the rate increase, and correspondingly P–Ta and R–T intervals became shorter as well. At such very fast rates the distance between the T and P waves of subsequent beats gets smaller, and these waves may even merge with each other. Many factors may cause the sinus tachycardia, it occurs most often as a physiological response to physical exercises, stress, fever, or may also result from congestive heart failure.

Sinus bradycardia is slow sinus rhythm less than 60 bpm, and occurs naturally during sleep. It is normal in children and athletes or may be a consequence of increased

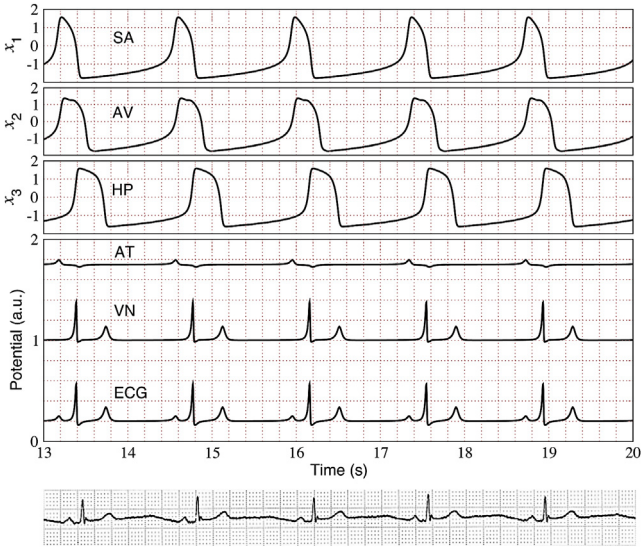

Fig. 9 – Calculated action potentials, muscle response and ECG at 43 bpm (bradycardia) and real patient's ECG [45].

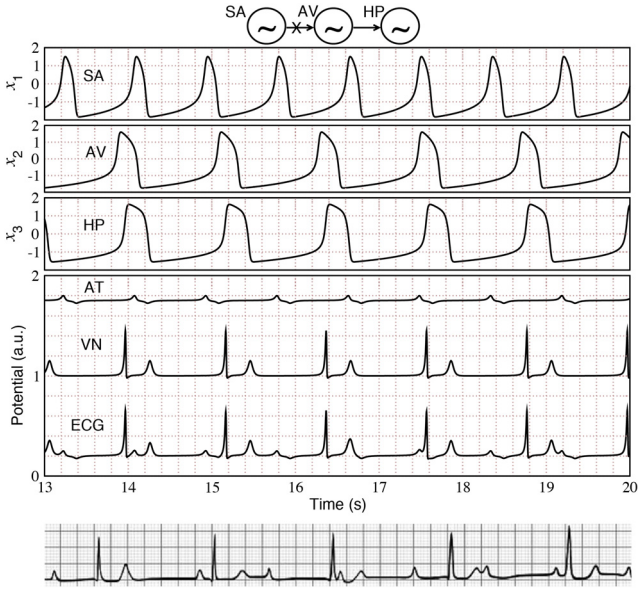

Fig. 10 – Calculated action potentials, muscle response and ECG at complete SA–AV block and real patient's ECG [46].

parasympathetic or vagal tone. Fig. 9 demonstrates the simulation results obtained at 43 bpm ($f_1 = 13$). The regular rhythm is also translated with same shape and rate from SA to AV and HP. It is seen on the obtained ECG that the P–Ta and R–T intervals are increased.

Though with decreasing rate pacemaker's action potential duration increases, the ratio between it and diastolic interval becomes smaller, as it seen from Figs. 7–9.

In the next computer experiments, we studied interactions among different parts of the heart, completely broken coupling between pacemakers.

Fig. 11 – Calculated action potentials, muscle response and ECG at complete AV–HP block and real patient's ECG [46].

Please cite this article in press as: E. Ryzhii, M. Ryzhii, A heterogeneous coupled oscillator model for simulation of ECG signals, Comput. Methods Programs Biomed. (2014), http://dx.doi.org/10.1016/j.cmpb.2014.04.009

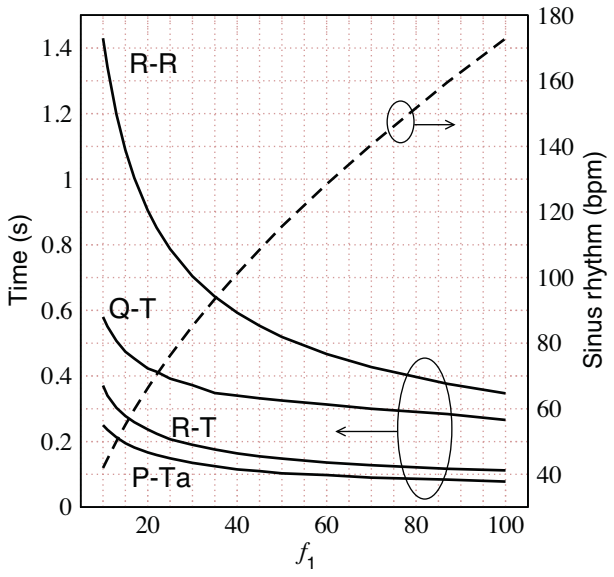

Fig. 12 – Dependences of R–R, Q–T, R–T, and P–Ta intervals (solid lines) and sinus rhythm (dashed line) on the parameter f_1.

Fig. 10 presents the result of simulation of complete SA–AV block at SA regular rhythm of 70 bpm. The SA action potential shapes and durations are normal, and P and Ta waves are normal accordingly. The AV node fires at its own rate of 50 bpm and the HP node synchronously follows the AV action potentials. In this case, atrial muscle operates at the rate of 70 bpm, while ventricles beat at slower rate of 50 bpm. The obtained ECG reflects this disturbance as atrial P and Ta waves and QRS complexes and T waves are unrelated in time.

Complete block between AV and HP pacemakers (Fig. 11) leads to independent operation of HP node at its own rate of 30 bpm with expanded action potentials, while normally coupled SA and AV nodes are beating at 70 bpm and their action potentials correspond to the normal case. Thus, we get independent normal action of atria and slow rate of ventricles.

In Figs. 10 and 11 one can observe the asynchrony of atrial and ventricular depolarization/repolarization processes represented by independent appearance of P and unmasked Ta waves on the one hand, and QRS complex and T wave on the other hand [31]. In all cases demonstrated in Figs. 7–11 we observe good conformity of simulated synthetic ECG with the presented clinical data.

Fig. 12 shows dependence of the obtained major ECG intervals on parameter f_1 which controls intrinsic frequency of the main oscillator. The R–R interval is the time between peaks of the neighboring R waves and related to the ventricular cycle. The Q–T interval is measured from the beginning of QRS complex to the end of T wave and represents the total duration of ventricular depolarization. For the rate of 70 bpm ($f_1 = 22$) we obtained the value of 0.41 s, which lays in the normal physiological range (0.3–0.45 s). Both the R–R and the Q–T intervals are usually being used in clinical practice to analyze patient's ECG.

Two additional intervals R–T and P–Ta shown in Fig. 12 were measured between corresponding peaks on the calculated ECG and represent the correlation between the depolarization and repolarization processes in atria and ventricles at different heart rates. All the calculated intervals are inversely proportional to the parameter f_1 in accordance with experimental findings. The calculated nonlinear dependence of sinus rhythm on f_1 is added for easy calculation of the former.

We mentioned in the introduction that there is a limited number of similar models generating artificial ECG signals with sets of ordinary differential equations [8,9,22,24]. In contrast to these models, we took into account macroscopic structure of cardiac conduction system and atrial and ventricular muscles. This allowed us to observe the interaction of the system elements such as different conduction blocks on the ECG (see Figs. 10 and 11). Using the proposed model with separate FHN systems for the description of depolarization and repolarization processes one can study appearance of the Ta wave and its input to the net ECG signal in different situations.

Implementation of the signal voltage derivative (transmembrane current) coupling between the SA and HP pacemakers and AT and VN muscles described by FHN type equations, respectively, allowed obtaining of realistic P–Ta and R–T intervals in the wide range of sinus rhythms (Fig. 12).

Inclusion of additional factors affecting the regular sinus rhythm, such as heart rate variability phenomena (respiratory arrhythmia) and low-frequency oscillations associated with Mayer waves, similar to the work by McSharry et al. [8] can further improve feasibility of our model.

5. Conclusion

We proposed a novel mathematical model of cardiac electrical system consisting of a network of heterogeneous oscillators described by nonlinear differential equations. We used modified van der Pol equations for the most important natural cardiac pacemakers (sinoatrial and atrioventricular nodes, and His–Purkinje system) connected with time-delay velocity coupling. To describe each of depolarization and repolarization processes individually in atrial and ventricular muscles, we utilized modified FitzHugh–Nagumo-type model, with stimulation current pulses produced by the related pacemakers. For solution of the system of delay differential equations describing the proposed oscillator model we developed a software in MATLAB environment utilizing special DDE23 function. Synthetic ECG waveforms are obtained as a combination of atrial and ventricular muscle signals.

Our model is capable to accurately reproduce realistic ECG characteristic to well known normal and pathological rhythms. The obtained results demonstrate that the proposed model is suitable to study global cardiac electrical activity. It allows investigation of the interactions between main parts of the heart, with possibility to utilize various models for pacemakers with different coupling types, as well as evaluation and comparison of underlying cardiac dynamics with widely used in clinical practice ECG patterns.

Please cite this article in press as: E. Ryzhii, M. Ryzhii, A heterogeneous coupled oscillator model for simulation of ECG signals, Comput. Methods Programs Biomed. (2014), http://dx.doi.org/10.1016/j.cmpb.2014.04.009

Conflict of interest

No conflict of interest.

REFERENCES

[1] U.R. Acharya, O. Faust, V. Sree, G. Swapna, R.J. Martis, N.A. Kadri, J.S. Suri, Linear and nonlinear analysis of normal and CAD-affected heart rate signals, Comput. Methods Prog. Biomed. 113 (2014) 55–68.
[2] T.Y. Ji, Q.H. Wue, Broadband noise suppression and feature identification of ECG waveforms using mathematical morphology and embedding theorem, Comput. Methods Prog. Biomed. 112 (2013) 466–480.
[3] A. Rosado-Muoz, J.M. Martez-Martez, P. Escandell-Montero, E. Soria-Olivas, Visual data mining with self-organising maps for ventricular fibrillation analysis, Comput. Methods Prog. Biomed. 111 (2013) 269–279.
[4] A.J. Pullan, M.L. Buist, L.K. Cheng, Mathematical modeling the electrical activity of the heart: from cell to body surface and back again, World Sci. (2005).
[5] F.B. Sachse, Computational Cardiology: Modeling of Anatomy, Electrophysiology, and Mechanics, Springer, New York, 2004.
[6] K.H. ten Tusscher, A.V. Panfilov, Modelling of the ventricular conduction system, Progr. Biophys. Mol. Biol. 96 (2008) 152–170.
[7] G. Plank, L. Zhou, J.L. Greenstein, S. Cortassa, R.L. Winslow, B. O'Rourke, N.A. Trayanova, From mitochondrial ion channels to arrhythmias in the heart: computational techniques to bridge the spatio-temporal scales, Philos. Trans. Roy. Soc. A 366 (2008) 3381–3409.
[8] P.E. McSharry, G. Clifford, L. Tarassenko, L.A. Smith, A dynamical model for generating synthetic electrocardiogram signals, IEEE Trans. Biomed. Eng. 50 (2003) 289–294.
[9] M. Gidea, C. Gidea, W. Byrd, Deterministic models for simulating electrocardiographic signals, Commun. Nonlin. Sci. Numer. Simul. 16 (2011) 3871–3880.
[10] N. Jafarnia-Dabanloo, D.C. McLernon, H. Zhang, A. Ayatollahi, V. Johari-Majd, A modified Zeeman model for producing HRV signals and its application to ECG signal generation, J. Theor. Biol. 244 (2007) 180–189.
[11] W. Thanom, R.N.K. Loh, Nonlinear control of heartbeat models, Syst. Cybern. Inform. 9 (2011) 21–27.
[12] J. Honerkamp, The heart as a system of coupled nonlinear oscillators, J. Math. Biol. 18 (1983) 69–88.
[13] S. Sato, S. Doi, T. Nomura, Bonhoeffer–van der Pol oscillator model of the sino-atrial node: a possible mechanism of heart rate regulation, Methods Inform. Med. 33 (1994) 116–119.
[14] R.L. Winslow, D. Cai, A. Varghese, Y-C. Lai, Generation and propagation of normal and abnormal pacemaker activity in network models of cardiac sinus node and atrium, Chaos Solit. Fract. 5 (1995) 491–512.
[15] M.G. Signorini, S. Cerutti, D. Di Bernardo, Simulation of heartbeat dynamics: a nonlinear model, Int. J. Bifurc. Chaos 8 (1998) 1725–1731.
[16] D. Di Bernardo, M.G. Signorini, S. Cerutti, A model of two nonlinear coupled oscillators for the study of heartbeat dynamics, Int. J. Bifur. Chaos 8 (1998) 1975–1985.
[17] K. Grudzinski, J.J. Zebrowski, Modeling cardiac pacemakers with relaxation oscillators, Physica A 336 (2004) 153–162.
[18] A.M. Dos Santos, S.R. Lopes, R.L. Viana, Rhythm synchronization and chaotic modulation of coupled van der Pol oscillators in a model for the heartbeat, Physica A 338 (2004) 335–355.
[19] M. Yoneyama, K. Kawahara, Coupled oscillator systems of cultured cardiac myocytes: fluctuation and scaling properties, Phys. Rev. E 70 (2004), 021904(1–9).
[20] A.M. Dos Santos, S.R. Lopes, R.L. Viana, Synchronization regimes for two coupled noisy Lienard-type driven oscillators, Chaos Solit. Fract. 36 (2008) 901–910.
[21] B.Z. Kaplan, I. Gabay, G. Sarafian, D. Safarian, Biological applications of the "filtered" van der Pol oscillator, J. Frank. Inst. 345 (2008) 226–232.
[22] Gois SRFSM, M.A. Savi, An analysis of heart rhythm dynamics using a three coupled oscillator model, Chaos Solit. Fract. 41 (2009) 2553–2565.
[23] M. Suchorsky, R. Rand, Three oscillator model of the heartbeat generator, Commun. Nonlin. Sci. Numer. Simul. 14 (2009) 2434–2449.
[24] S. Das, K. Maharatna, Fractional dynamical model for the generation of ECG like signals from filtered coupled van-der Pol oscillators, Comput. Methods Prog. Biomed. 112 (2013) 490–507.
[25] F.A. Roberge, P. Bhereur, R.A. Nadeau, A cardiac pacemaker model, Med. Biol. Eng. 9 (1971) 3–12.
[26] O. Kongas, R. von Hertzen, J. Engelbrecht, Bifurcation structure of a periodically driven nerve pulse equation modeling cardiac conduction, Chaos Solit. Fract. 10 (1999) 119–136.
[27] J.J. Zebrowski, K. Grudzinski, T. Buchner, P. Kuklik, J. Gac, G. Gielerak, P. Sanders, R. Baranowski, Nonlinear oscillator model reproducing various phenomena in the dynamics of the conduction system of the heart, Chaos 17 (2007), 015121(1–10).
[28] H. Sheheitli, R. Rand, Origin of arrhythmias in a heart model, Commun. Nonlin. Sci. Numer. Simul. 14 (2009) 3707–3714.
[29] B. Van der Pol, J. van der Mark, The heartbeat considered as a relaxation oscillation, and an electrical model of the heart, Philos. Mag. 6 (1928) 763–775.
[30] E. Ryzhii, M. Ryzhii, Modeling of heartbeat dynamics with a system of coupled nonlinear oscillators, Commun. Comput. Inform. Sci. 0404 (2013) 157–165.
[31] V. Fuster, R.A. Walsh, R.A. Harrington, Hurst's the Heart, 13th ed., McGrow Hill Medical, New York, 2011.
[32] J. Malmivuo, R. Plonsey, Bioelectromagnetism, Oxford University Press, New York, 1995.
[33] C. Morris, H. Lecar, Voltage oscillations in the barnacle giant muscle fiber, Biophys. J. 35 (1981) 193–213.
[34] D. Postnov, S.K. Han, S. Kook, Synchronization of diffusively coupled oscillators near the homoclinic bifurcation, Phys. Rev. E 60 (1999) 2799–2807.
[35] S. Wirkus, R. Rand, The dynamics of two coupled van der Pol oscillators with delay coupling, Nonlin. Dyn. 30 (2002) 205–221.
[36] M.R. Boyett, H. Honjo, I. Kodama, The sinoatrial node, a heterogeneous pacemaker structure, Cardiovasc. Res. 47 (2000) 658–687.
[37] F.L. Meijler, M.J. Janse, Morphology and electrophysiology of the mammalian atrioventricular node, Physiol. Rev. 68 (1988) 608–647.
[38] P.A. Boyden, M. Hirose, W. Dun, Cardiac Purkinje cells, Heart Rhythm 7 (2010) 127–135.
[39] R. FitzHugh, Impulses and physiological states in theoretical models of nerve membrane, Biophys. J. 1 (1961) 445–466.
[40] J. Nagumo, S. Arimoto, S. Yoshizawa, An active pulse transmission line simulating nerve axon, Proc. IRE 50 (1962) 2061–2070.
[41] J.M. Rogers, A.D. McCulloch, A collocation-Galerkin finite element model of cardiac action potential propagation, IEEE Trans. Biomed. Eng. 41 (1994) 743–757.
[42] L.F. Shampine, S. Thompson, Solving DDEs in MATLAB, Appl. Numer. Math. 37 (2001) 441–458.

Please cite this article in press as: E. Ryzhii, M. Ryzhii, A heterogeneous coupled oscillator model for simulation of ECG signals, Comput. Methods Programs Biomed. (2014), http://dx.doi.org/10.1016/j.cmpb.2014.04.009

[43] J. Kierzenka, L.F. Shampine, S. Thompson, Solving Delay Differential Equations With DDE23. http://www.mathworks.com/dde_tutorial
[44] R.J. Bauer, G. Mo, W. Krzyzanski, Solving delay differential equations in S-ADAPT by method of steps, Comput. Methods Prog. Biomed. 111 (3) (2013) 715–734.
[45] Illustrated Book on Electrocardiography. Cardiophile MD, http://cardiophile.org/electrocardiography/
[46] ECG Library, http://lifeinthefastlane.com/ecg-library/

Please cite this article in press as: E. Ryzhii, M. Ryzhii, A heterogeneous coupled oscillator model for simulation of ECG signals, Comput. Methods Programs Biomed. (2014), http://dx.doi.org/10.1016/j.cmpb.2014.04.009